DIAGNOSTIC NUCLEAR MEDICINE

Spatial and Temporal Quantitation of Plane Thallium Myocardial Images

Denny D. Watson, Norman P. Campbell, Eileen K. Read, Robert S. Gibson, Charles D. Teates, and George A. Beller

University of Virginia Medical Center, Charlottesville, Virginia

A computer method has been developed to determine the relative initial uptake and segmental washout rates of thallium-201 from sequential myocardial images. Initial images in multiple projections are obtained at 10 min after thallium-201 injection, and delayed images 2–3 hr after injection. A modified interpolative method was used to construct a background reference plane, and net myocardial counts above this reference plane were determined from multiple count profiles. Washout rates were determined by linear regression of time-activity curves constructed from the sequential images. In this approach, both relative temporal as well as relative spatial quantitation is performed. Data from 25 normal subjects were used to establish numerical criteria and normal ranges for relative focal defects and abnormal segmental washout slopes. Normal ranges were set to include the 90-percentile limits of the distribution of values obtained from the normal population. From these values we derived a quantitative criterion for thallium scan interpretation that can be used for analysis and interpretation of scintigrams in clinical situations.

J Nucl Med 22: 577–584, 1981

The need for a more quantitative approach to thallium-201 myocardial imaging is currently recognized. Quantitation can be performed by comparing the relative activity of different myocardial segments in the same image (spatial) or by determining the relative activity of the same segment as a function of time (temporal). Temporal quantitation is required to characterize thallium redistribution, which is commonly observed (*1–7*).

The redistribution of thallium in delayed images occurs because a normal myocardial segment has a characteristic pattern of thallium uptake and washout differing from that of an abnormal myocardial segment. The initial uptake of thallium is nearly proportional to regional myocardial blood flow (*1, 8, 9*), and following the initial myocardial extraction of thallium there is continuous exchange of thallium across the myocardial cell membrane (*10–12*). Within 2 or 3 hr after injection, a potentially different concentration of thallium results from an exchange equilibrium determined by a balance between continuous cellular uptake and efflux of thallium. Thus the delayed thallium distribution reflects, rather than blood flow, an equilibrium condition determined by intracellular thallium exchange. The determination of the entire uptake and washout curve may, therefore, provide more complete characterization of myocardial blood flow and cellular integrity. This paper describes a method utilizing both relative temporal as well as relative spatial quantitation in order to capitalize on the kinetic as well as the static information intrinsic to thallium studies.

Received July 24, 1980; revision accepted March 30, 1981.

For reprints contact: Denny D. Watson, PhD, Div. of Nuclear Imaging, Univ. of Virginia Medical Center, Box 468, Charlottesville, VA 22908.

METHODS

Background subtraction. In Tl-201 myocardial images, a significant fraction of the total counts within a myocardial target region arise from "background"—or,

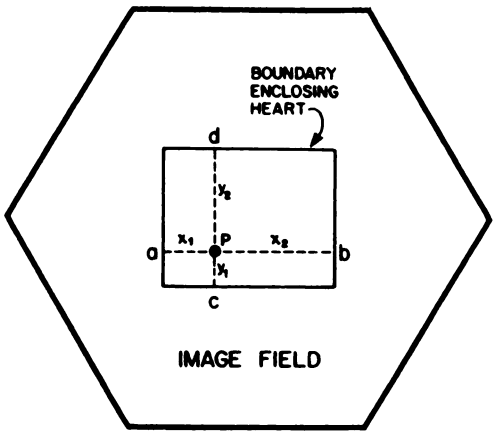

FIG. 1. Myocardial image field with computer-defined boundary circumscribing heart. Background value B at point P is computed according to formula given in text.

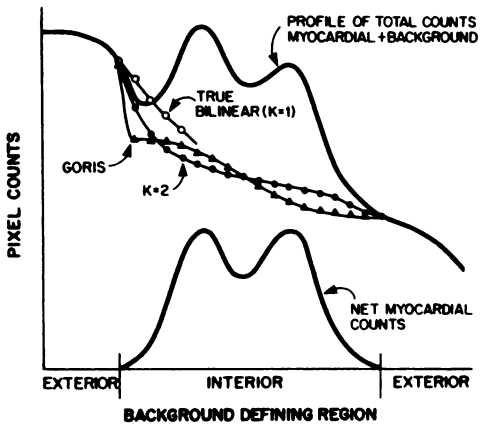

FIG. 2. Illustrating a single profile slice through a background reference plane, as generated by the Goris formula, by our modified formula with k = 2, and again with k = 1. The last is called "true bilinear" since it amounts to using edge-weighting factors inversely proportional to the distance from the interior point to the background-defining region. Formula with k = 2 provides smooth roll-off from region of high exterior background at left, but eliminates edge discontinuities.

more correctly, "tissue crosstalk" (*19*). The distribution of this crosstalk is certainly nonuniform and cannot be adequately treated as a constant (*13*); moreover, it changes with time. Our method of separating tissue cross talk from myocardial activity follows that described by Goris et al. (*13*), utilizing a nonuniform background reference plane but with a modified formula for computing background elements. The quantitative results will be based on residual myocardial counts above the background reference plane; they are therefore dependent upon the particular method of background subtraction.

The method of generating the background reference plane is as follows. A boundary region is chosen, enclosing the heart (Fig. 1). All image points outside this boundary region are defined to be background. The background in the interior region at point P must be computed. Let a, b, c, and d be the number of image counts found on the orthogonal boundary points that are respectively at distances x_1, x_2, y_1, and y_2 from the point P. The background B at the interior point P is computed from the symmetrically weighted average:

$$B = \frac{w_a a + w_b b + w_c c + w_d d}{w_a + w_b + w_c + w_d}.$$

The weighting factors w_a, w_b, w_c, w_d are as follows, where k = 2:

$$w_a = \frac{x_2}{x_1} + k, \quad w_b = \frac{x_1}{x_2} + k,$$

$$w_c = \frac{y_2}{y_1} + k, \quad w_d = \frac{y_1}{y_2} + k.$$

These weight factors differ from the formula of Goris et al. (*13*) in two respects. First, the weight factors are inversely related to the distances between the background point P and the boundary points. This eliminates discontinuities at the boundary region, which would sometimes occur with the original weight functions. Second, the constant k has been introduced to cause a more rapid fall-off of the background reference plane as it moves beneath the heart away from a region of intense extracardiac activity, such as the liver or spleen. The value k = 2 was chosen because it produces a fall-off with approximately the same spatial frequency as would be encountered at the borders of an isolated organ, thus preventing erroneous extrapolation of isolated organ activity into the computed background plane (Fig. 2).

The background subtraction is shown in Fig. 3. A separate background is generated for each image. The displayed images are unsmoothed, but background is generated from a smoothed image and subtracted from

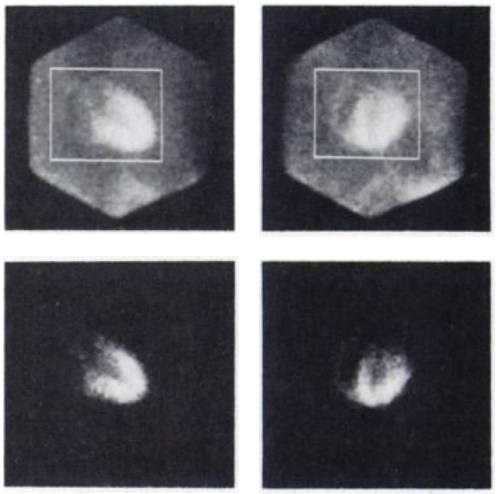

FIG. 3. Upper images are anterior (L) and 45° LAO (R) Tl-201 myocardial images. Computer-generated region around the heart has been defined. Lower images show net myocardial counts following subtraction of computer-generated background plane. Value of weak noise pattern in lower images is discussed in the text.

the unsmoothed raw image. Such a subtraction leaves a random pattern of residual counts outside of the myocardium reflecting Poisson statistical noise, thus providing for a quick visual check of the correctness of the background reference plane. If the background is too high or too low in a certain region, that region will either have, respectively, no residual counts or excessive residual counts.

Quantitation. Regional thallium activity on anterior and 45° left anterior oblique projections is measured on images obtained at 10 min after injection and on delayed images at approximately 1 hr, and again at 2–3 hr, after injection. The initial and delayed images should be identically positioned, and image overlap is accomplished by a computer program (*14*). Briefly, the computer initially calculates the two-dimensional centroid of each of the myocardial images in the sequence, and repositions each of the images so that the image centroids are located at the center of the image matrix. An iterative translation of the positions of the delayed images is then performed to maximize the cross-correlation coefficient between the initial image and the later images. This aligns the sequential images according to a two-dimensional, least-squares criterion.

The computer next generates four profile slices across each myocardial image; these are positioned to quarter the myocardial image (Fig. 4). The residual myocardial image is smoothed once before the slice is taken. The slices are of a single pixel element width, but actually represent nine-pixel averages due to the smoothing operation. The quantitation in each thallium image is based upon the peaks of the four profile slices as they pass across the myocardial rim in the selected myocardial segment, as shown in Fig. 5.

All data were stored by computer in a 64X 64 matrix.

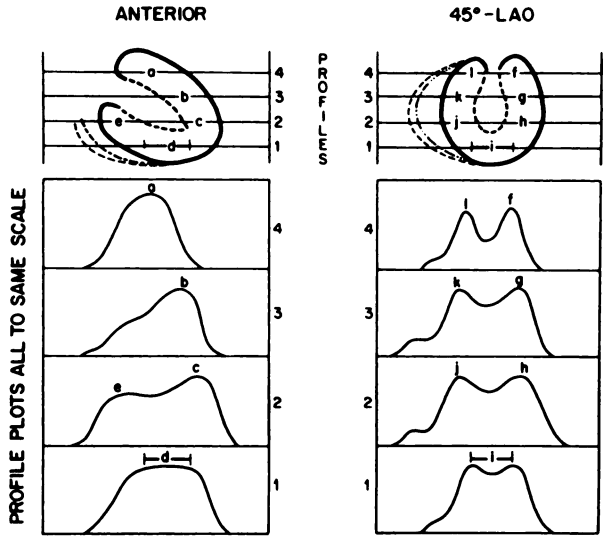

FIG. 4. Illustrating placement of profile slices on net myocardial images. Profiles below are appropriately numbered and lettered for reference. Peaks characterize Tl-201 behavior.

All thallium images were displayed uniformly on a special computer gray scale designed to compensate for the intrinsically logarithmic response of human visual perception (*22*). Both the raw image and its net counterpart after interpolative background subtraction were displayed on the same standardized gray scale, and no form of threshold suppression or contrast enhancement was used.

For this study, data were obtained from five segments

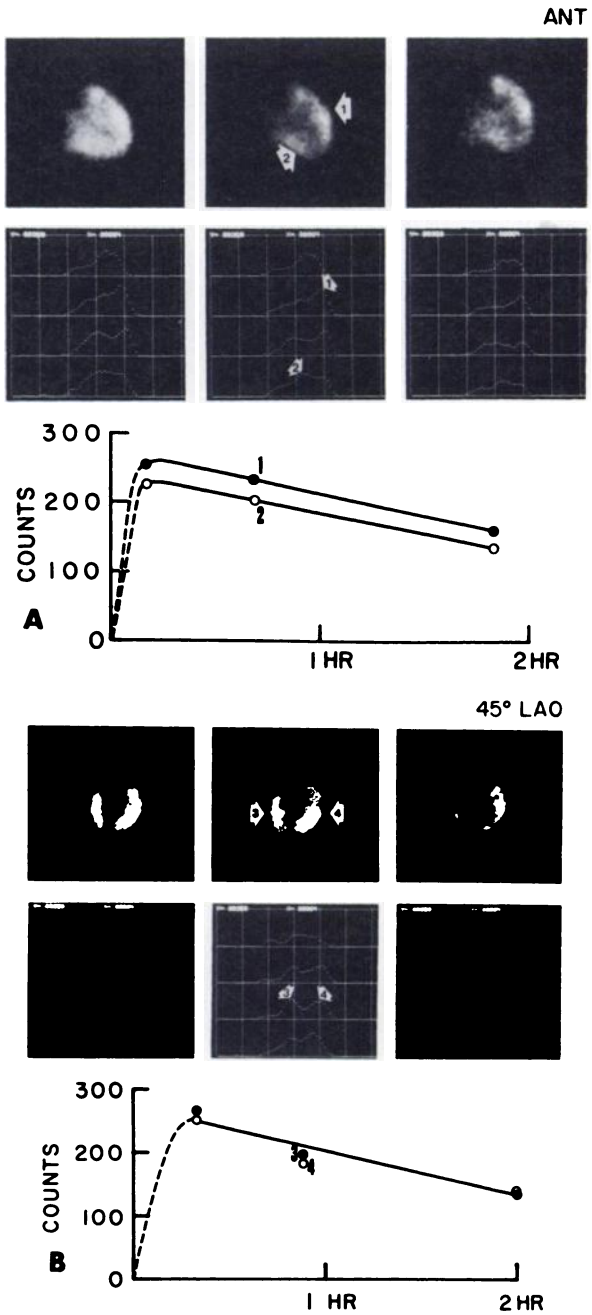

FIG. 5. (A) Three sequential Tl-201 images, anterior projection, with slice profiles below. Time-activity curves, 1 and 2, are for regions indicated by arrows, and pattern was similar elsewhere in this normal heart. (B) Similar sequence in 45° LAO; arrows indicate regions selected for accompanying plots.

of the left ventricle. These segments were the inferior and anterolateral wall as viewed in the anterior projection, and the anteroseptal, posterolateral, and inferoapical walls as viewed from the 45° LAO projection. Data were also obtained from the right ventricle as viewed in the 45° LAO projection. Right-ventricular activity was determined from the profile having the highest counts per pixel as it crossed the right ventricle.

Selection of patients for normal standards. Twenty-five normal patients were selected for determination of normal standards. Sixteen (three being females) had undergone coronary arteriography and left ventriculography. In all 16 (Group A), the coronary arteries were without significant narrowings and the left ventricle contracted normally. Four of the 16 had abnormal resting electrocardiograms (nonspecific ST-T wave changes in two; right bundle branch block in one; short PR interval in one). Eight of these patients were receiving propranolol at the time of perfusion imaging. This group achieved a mean maximum predicted heart rate of (83 ± 11)% at a mean rate-pressure product of $22 \pm 6 \times 10^3$.

The nine patients comprising Group B were chosen from the same population but did not undergo arteriography. These were selected by the following criteria: (a) age less than 50 yr; (b) no past history of hypertension; (c) normal physical examination; (d) normal resting electrocardiogram; (e) normal chest radiogram; (f) normal graded-exercise treadmill test;* and (g) normal myocardial distribution of Tl-201 on post-exercise images. The criteria for normality were derived from Group A patients. This group achieved a mean maximum predicted heart rate of (89 ± 2)% at a mean rate-pressure product of $27 \pm 3 \times 10^3$.

Measurements of activity from the initial anterior and 45° LAO images were used to assess the initial distribution of Tl-201. In those regions crossed by two profiles, both the highest and the mean of the peak activities were recorded. The sequential images were used to produce time-activity curves for each region of the heart. Changes in counts/pixel with time were measured using the same profiles for each sequential image. Each time-activity curve was defined by three points. From these data, lines of best fit were determined by linear least-squares regression analysis. The half-time ($t_{1/2}$) for Tl-201 activity and for the fractional washout coefficient (k) were calculated from the slopes and Y-axis intercepts of the linear regression lines using the following equations:

$$k = \frac{\text{slope}}{\text{intercept}}, \qquad t_{1/2} = -\frac{1}{2k}.$$

Linear regression lines, instead of exponential curves, were chosen to represent this phase of the washout curve for two reasons: First, to simplify the analysis. Second, in the time interval we are using, the uptake and washout curve passes through an inflection point that creates a zero in the second derivative. In this time interval, the linear curve segment can be thought of as a Taylor-series expansion that is valid to third order due to the vanishing of the second derivative. Thus, the linear expansion would actually represent a closer mathematical approximation to the curve's shape than would a monoexponential function.

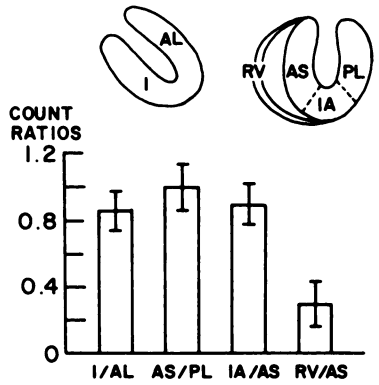

FIG. 6. Ratios between net Tl-201 activity in various regions of heart, as indicated at bottom. Standard deviation is shown for each bar.

All results are shown as the mean plus or minus one standard deviation (s.d.).

RESULTS

Regional distribution. The total number of events recorded in the first 10-min imaging periods averaged 362 ± 75 × 10^3 counts in the anterior projection, and 359 ± 76 × 10^3 counts in the 45° LAO. By the third images (2.5 -3 hr), the mean activity in the 10-min imaging intervals for the two views had fallen to 289 ± 59 × 10^3 and 292 ± 57 × 10^3, respectively.

Figure 6 summarizes the regional relative distribution of Tl-201, determined between various myocardial segments from the early images in the 16 patients comprising Group A. The ratios of activities obtained from any position on the anteroseptal and posterolateral walls were essentially unity. The inferior wall, viewed in the anterior projection, had an average 10% less activity than the anterolateral wall, due to absorption by the overlying right-ventricular cavity. In the 45° LAO projection, the minimum activity in the inferoapical segment viewed was similarly about 10% less than that found in the anteroseptal and posterolateral walls.

The ratios of activity found within or between myocardial regions were independent of the rate-pressure product achieved with exercise or of the duration of exercise.

The possibility of oversubtraction by the background reference plane was assessed in another group of 50 patients with transmural myocardial infarction who underwent thallium scintigraphy. In thallium scan segments corresponding to infarct locations, the thallium

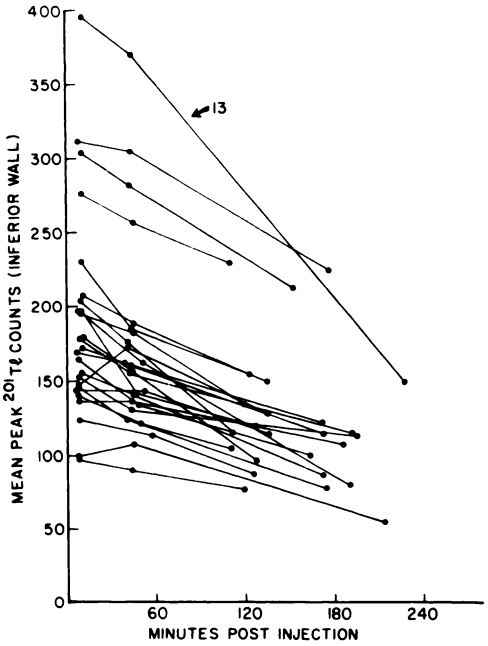

FIG. 7. Normal time-activity curves from the inferior wall of left ventricle. One subject had atypically high count density and rapid washout throughout heart, but catheterization was uninformative.

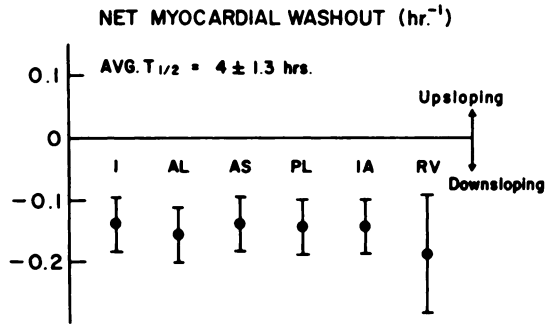

FIG. 8. Washout coefficient, k, for various myocardial segments. I = inferior, AL = anterolateral, AS = anteroseptal, PL = posterolateral, RV = right ventricle. Negative sign represents net loss of thallium over 2–3-hr interval. The error bars are standard deviations.

activity above the reference plane averaged (18 ± 9)% of the thallium activity observed in adjacent myocardium. A negative residual count was not observed in any segment.

Time-activity curves. These were drawn using the results from patients in both Groups A and B. Since Group B patients were "normal" with respect to spatial distribution of thallium in the postexercise scintigrams, they have been included with Group A patients for determination of normal values for segmental thallium washout. Figure 7 illustrates findings obtained from the profiles crossing the inferior wall of the left ventricle in the anterior projection. The slopes obtained from least-squares fitting of the three points were negative for all segments in all patients. In 78% of the regions studied, Tl-201 activity was greatest in the first image. In 8% the activity was found to be equal in the first and second images, and in 14% the second image showed more activity than the first.

The slopes obtained for the various myocardial segments, including the right ventricle, are summarized in Fig. 8. Where two profiles crossed a myocardial region, slope measurements were obtained both from the highest values and also from the mean values. The mode of measuring did not significantly alter the values for mean slope, $t_{1/2}$, or k. There was no significant difference in the slopes obtained from any of the myocardial segments.

The washout rate (slope) in each region of the heart correlated moderately (r = 0.6 in all regions) with net myocardial counts, indicating a tendency to observe more rapid washout in cases with higher initial net myocardial uptake. The $t_{1/2}$ for net myocardial washout similarly correlated moderately well with the rate-pressure product at peak exercise (r = 0.6).

Criteria for clinical interpretation. An abnormal myocardial segment is identified by: (a) a focal defect on the initial image, (b) relative redistribution on the delayed images, or (c) abnormal washout in the delayed images. An initial image is considered abnormal if it presents a focal area of decreased uptake greater than 25% of the uptake in adjacent or contralateral myocardial regions. The 25% criterion represents more than 1.6 standard deviations from the mean of the normal population, and therefore represents a 90-percentile discriminant. An exception is noted for a persistent decrease in the inferior wall observed in the anterior projection, which should be considered significant only if it exceeds 35%. This allows for absorption in the overlying right-ventricular chamber. The apex of the left ventricle obtains a similar exception because of normal variant apical thinning. A profile crossing the aortic outflow track will indicate decreased activity, which should not be interpreted as a focal defect. The position of the aortic outflow track will vary somewhat with the cardiac rotation. In female patients, photon attenuation through breast tissue can cause significant shadows that can be recognized on the unprocessed scintiphotos.

Redistribution is said to occur when the ratio of two different myocardial segments changes between the initial and delayed images. The classical form of redistribution is that of an abnormal myocardial segment, which initially accumulates less thallium and clears more slowly compared with an adjacent normal myocardial segment, which accumulates more thallium initially and clears more rapidly. An abnormal myocardial segment may also have decreased initial uptake, with continuously increasing thallium uptake in the delayed images. In some cases there are no normal myocardial segments for comparison. In such situations, the apparent redistribution patterns may be bizarre and difficult to interpret.

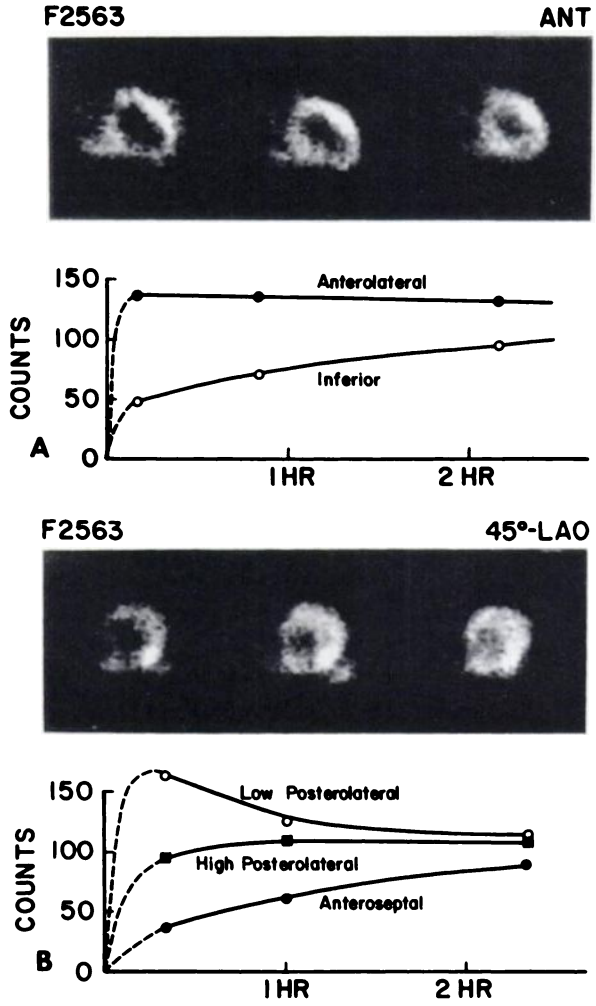

FIG. 9. (A) anterior images and time-activity curves for left ventricular regions indicated from patient with three-vessel disease. Inferior region shows initial defect, redistribution, and abnormally increasing uptake; anterolateral region has borderline (flat) washout. (B) same patient, 45° LAO. Top curve shows normal uptake and washout; both of other curves demonstrate initial defect, redistribution, and abnormal washout.

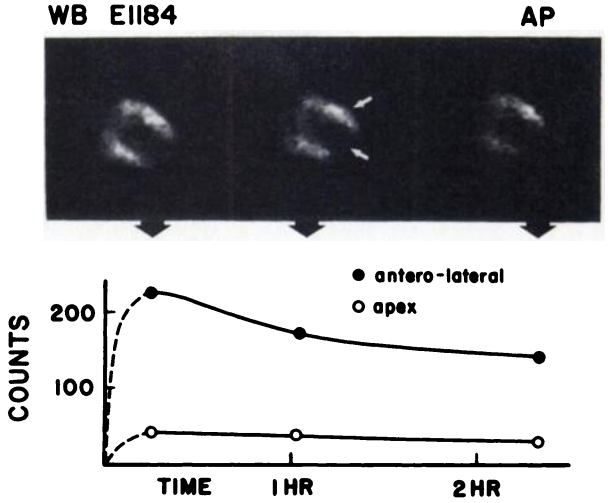

FIG. 10. Postexercise study in patient with prior myocardial infarction. Time-activity curves are from normal anterolateral region (upper arrow) and from scarred apex (lower arrow).

These cases can normally be identified by observing abnormal washout in all myocardial segments, as discussed in the following paragraph.

The determination of washout slopes in each myocardial segment forms an absolute criterion to identify normal segments and does not require a normal segment for comparison. Following exercise stress, a myocardial segment that fails to decrease in net thallium concentration in the 2–3 hr delayed images is considered to be abnormal. This criterion is more than two standard deviations from the distribution observed in the normal population. The use of upslope against downslope provides a discriminant that requires no mathematical computations, and encompasses the normal physiologic variability in net washout rate. The use of all three interpretive criteria is illustrated in Figs. 9 and 10.

These criteria have been applied to an independent group of 140 patients referred for evaluation of chest pain. This study (reported in this issue) yielded a 91% sensitivity and 90% specificity for the detection of significant coronary artery disease (*16*).

DISCUSSION

In this paper, a systematic approach to the relative quantitation of myocardial thallium-201 scintigrams is described, and objective standards for the interpretation of exercise thallium scans have been derived from a population of normal individuals. This technique employs relative temporal as well as relative spatial quantitation and provides a basis from which to evaluate abnormalities in the transport of thallium as well as abnormal initial uptake. Temporal quantitation uses the initial thallium uptake in each myocardial segment as a control value for comparison with the same segment in delayed images, and does not require the presence of a normal myocardial segment for comparison.

The background reference plane forms the basis of this method and is a first-order approximation that ignores higher order effects from self-absorption and Compton scattering. This approximation was deliberately chosen to achieve simplicity and reproducibility. A potential problem associated with generating a background reference plane beneath the heart has been pointed out by Narahara et al. (*17*) and by Beck et al. (*18*), who measured the residual activity following intravenous thallium administration in dogs after removing the heart and replacing it either by a water absorber or another canine heart containing no myocardial thallium activity. Both groups observed photon-deficient regions or "dips" in the profile slices taken across the myocardial region after removal of the heart. This effect is attributable to displacement of background-producing tissues and photon absorption by the heart and suggests that the refer-

ence-plane method as described above would result in consistent oversubtraction of background. This was not observed in the human studies, as indicated by the following observations. First, in the group of patients having large transmural myocardial scars, the net residual activity in the infarct region averaged 18% of the activity in normally perfused regions. Thus, even in the presence of extensive myocardial scars, slight net positive counts above the background reference plane are observed, revealing no evidence of over-subtraction. Second, systematic over-subtraction of background would alter the apparent washout rates in different myocardial regions. This would be true particularly for the washout rate from the right ventricle, which is very near the background level and is extremely sensitive to the amount of background subtracted. In our normal human subjects, the washout rates were identical in all myocardial regions of each individual including the right ventricle. Introducing a dip in the background function would have caused anomalous discrepancies to appear in the apparent washout rates. Third, in our normal subjects a homogeneous distribution of net myocardial counts was observed, and it would have become anomalously inhomogeneous if a more highly structured background were used.

The differences between the findings in our human subjects and in the animal models with removal of the hearts could in part be anatomic, but more likely is because much of the tissue crosstalk that comprises the "background" actually arises from Compton scattering of the low-energy photons originating from adjacent myocardial activity and scattered into the target's solid angle. This is a major source of tissue crosstalk in imaging of decreased areas of activity, and it was eliminated in the animal models by removal of the heart.

In contrast to other recent methods (*15*, *20*, *21*), we have chosen to use horizontal profile slices uniformly spaced across the heart, rather than individually selected myocardial segments, or circumferential or radial profiles. In our approach, the profile slices are positioned by the computer without regard to the angle of orientation of the heart. The position of each slice across the myocardium is automatically marked by the computer so that the interpreter can immediately recognize the exact position of the sampled myocardial segment and relate that to the corresponding profile peak. Identical positioning of sampled regions in sequential images is achieved by the computer program, which automatically repositions the sequential images to achieve image overlay. This technique results in an operator-independent analysis, and the resulting standardization and reproducibility of results is considered to be of paramount importance to any quantitative approach.

The average peak count density in the myocardial rim is used as the quantitative index of thallium uptake because it imposes no computational problems and represents a quantitative equivalent of the subjective criteria used for scan interpretation. The alternative use of areas beneath profile curves would have a statistical advantage but would suffer from dependence on the anatomic configuration of the ventricle and the relative orientation of the profile slice as well as on the method of choosing integration limits.

The number of profile slices taken across the heart can be varied. We have chosen four slices as a matter of convenience. On a normal-sized heart, this results in myocardial rim samples' being spaced at approximately 1.6-cm intervals. The profile slices represent approximately 0.8 cm^2 spatial averages. The use of smaller and more finely spaced samples around the myocardial rim tends to generate more data than can be assimilated easily by the interpreter, and it increases the likelihood of random errors.

The choice of imaging times is based upon studies of the myocardial kinetic transport of thallium-201 (*12*). The initial myocardial extraction of thallium-201 from the blood is quite rapid, with extraction of most of the thallium during the first capillary transit following injection. Subsequent redistribution begins immediately and is the result of continuous bidirectional exchange of thallium across the myocardial cell membrane. Thallium is injected before the termination of exercise so that there will be about 1 min to allow for the initial extraction to occur during exercise. The initial myocardial distribution of thallium will then reflect the blood-flow distribution during exercise and not be affected by rapid changes in myocardial blood flow that may occur following termination of exercise. After the initial extraction of thallium is complete, the rate of thallium redistribution will be limited by the transport rate across the myocardial cell membrane. The exchange process is characterized by a half-time of approximately 1 hr. The choice of a 2–3 hr interval between the initial and delayed images represents two to three half-times in the process of thallium redistribution towards a final equilibrium concentration. Thus, 2–3 hr should be a nearly optimal time at which to characterize the redistribution process.

FOOTNOTE

* All achieved at least 85% of the maximum predicted heart rate for their age and sex. None had ST-segment displacement with exercise (<1 mm displacement 0.08 sec after the J point).

ACKNOWLEDGMENT

We are grateful for the outstanding technical assistance of Gayle Petroff and Robin Waterfield. Supported in part by USPHS Grant HL-26205-01 and a Grant-in-Aid (76-942) from the American Heart Association.

REFERENCES

1. POHOST GM, ZIR LM, MOORE RH, et al: Differentiation of transiently ischemic from infarcted myocardium by serial

imaging after a single dose of thallium-201. *Circulation* 55: 294-302, 1977
2. BELLER GA, WATSON DD, ACKELL P, et al: Time course of thallium-201 redistribution after transient myocardial ischemia. *Circulation* 61:791-797, 1980
3. POHOST GM, OKADA RD, O'KEEFE DO, et al: Thallium redistribution in dogs with severe coronary artery stenosis of fixed caliber. *Circ Res* 48:439-466, 1981
4. BERGER BC, WATSON DD, BURWELL LR, et al: Redistribution of thallium at rest in patients with stable and unstable angina and the effect of coronary artery bypass surgery. *Circulation* 60:1114-1125, 1979
5. GEWIRTZ H, BELLER GA, STRAUSS HW, et al: Transient defects of resting thallium scans in patients with coronary artery disease. *Circulation* 59:707-713, 1979
6. GIBSON RS, TAYLOR GJ, WATSON DD, et al: Prognostic significance of resting anterior thallium-201 defects in patients with inferior myocardial infarction. *J Nucl Med* 21:1015-1021, 1980
7. SCHWARTZ JS, PONTO R, CARLYLE P, et al: Early redistribution of thallium-201 after temporary ischemia. *Circulation* 57:332-335, 1978
8. WEICH HF, STRAUSS HW, PITT B: The extraction of thallium-201 by the myocardium. *Circulation* 56:188-191, 1977
9. NIELSEN AP, MORRIS KG, MURDOCK R, et al: Linear relationship between the distribution of thallium-201 and blood flow in ischemic and nonischemic myocardium during exercise. *Circulation* 61:797-801
10. WATSON DD, BELLER GA, IRVING JF, et al: A kinetic model for thallium myocardial redistribution. *J Nucl Med* 19:680-681, 1978 (abst)
11. WATSON DD, BELLER GA, BERGER BC: The mechanism of thallium-201 redistribution. *Am J Cardiol* 43:357, 1979 (abst)
12. BELLER GA, WATSON DD, POHOST GM: Kinetics of thallium distribution and redistribution: clinical applications in sequential myocardial imaging. In *Cardiovascular Nuclear Medicine*. H. William Strauss, B. Pitt, A. E. James, Jr., Eds. St. Louis, C. V. Mosby, 1979, pp 225-242
13. GORIS ML, DASPIT SG, MCLAUGHLIN P, et al: Interpolative background subtraction. *J Nucl Med* 17:744-747, 1976
14. READ ME, WATSON DD, READ EK, et al: A method for automatic overlapping of sequential scintiphoto images. *J Nucl Med* 21:P61, 1980 (abst)
15. BUROW RD, POND M, SCHAFER AW, et al: "Circumferential profiles:" a new method for computer analysis of thallium-201 myocardial perfusion images. *J Nucl Med* 20: 771-777, 1979
16. BERGER BC, WATSON DD, TAYLOR GJ, et al: Quantitative thallium-201 exercise scintigraphy for detection of coronary artery disease. *J Nucl Med* 22:585-593, 1981
17. NARAHARA KA, HAMILTON GW, WILLIAMS DL, et al: Myocardial imaging with thallium-201: an experimental model for analysis of the true myocardial and background image components. *J Nucl Med* 18:781-786, 1977
18. BECK JW, TATUM JL, COBB FR, et al: Myocardial perfusion imaging using thallium-201: a new algorithm for calculation of background activity. *J Nucl Med* 20:1294-1300, 1979
19. GORIS ML: Nontarget activities: can we correct for them? *J Nucl Med* 20:1312-1314, 1979
20. VOGEL RA, KIRCH DL, LEFREE MT, et al: Thallium-201 myocardial perfusion scintigraphy: results of standard and multi-pinhole tomographic techniques. *Am J Cardiol* 43: 787-793, 1979
21. MEADE RC, BAMEAH VS, HORGAN JD, et al: Quantitative methods in the evaluation of thallium-201 myocardial perfusion images. *J Nucl Med* 19:1175-1178, 1978
22. WATSON DD, LEIDHOLT ZEM, BELLER GA, et al: Defect perception in myocardial perfusion images. *J Nucl Med* 21: P61-P62, 1980 (abst)